

# Current Sensorless Model Predictive Torque Control Based on Adaptive Backstepping Observer for PMSM Drives

QINGFANG TENG<sup>1</sup>, JIANYONG BAI<sup>1</sup>, JIANGUO ZHU<sup>2</sup>, YOUGUANG GUO<sup>2</sup>

<sup>1</sup>Department of Automation and Electrical Engineering  
Lanzhou Jiaotong University  
Lanzhou, Gansu, 730070  
P.R.CHINA

<sup>2</sup>Faculty of Engineering and Information Technology  
University of Technology Sydney  
Sydney, NSW, 2007  
AUSTRALIA

tengqf@mail.lzjtu.cn <http://www.lzjtu.edu.cn>

*Abstract:* - A novel adaptive backstepping observer is proposed and model predictive torque control (MPTC) strategy is considered for three-phase permanent magnet synchronous motor (PMSM) drives without any current sensor. Generally, instantaneous stator currents are required for successful operation of MPTC. If the stator current sensors fail, the most common technique for reconstructing stator currents mainly focuses on using information from a single current sensor in the DC-link of an inverter. Nevertheless, the existence of immeasurable regions in the output voltage hexagon results in that the three-phase currents will not be reliably detected since one or more of the active state vectors are not applied long enough to insure accurate measurements. In addition, the technique may suffer from the very noisy of DC-link current feedback. To avoid these drawbacks, making use of the technique of adaptive backstepping, a novel observer is proposed. The designed observer can be capable of concurrent estimation of stator currents and resistance under the assumption that rotor speed and inverter output voltage as well as DC-link voltage are available for measurement. Stability and convergence of the observer are analytically verified based on Lyapunov stability theory. In order to reduce the torque & flux ripples and improve drives control performance, MPTC strategy is employed. The proposed algorithm is less complicated and its implement is relatively easy. It can ensure that the whole drives system achieves satisfactory torque & speed control and strong robustness. Extensive simulation validates the feasibility and effectiveness of the proposed scheme.

*Key-Words:* - Model predictive torque control; Permanent magnet synchronous motor; Sensorless; Adaptive backstepping observer

## 1 Introduction

The electrical drive systems of modern automotive and aerospace along with other important fields must be required to be high reliable and safe. Due to a variety of complex factors, potential failures are often inevitable. Once the electrical drive is out of order, if repair and maintenance cannot be completed on the spot, this will result in the system to stop working and cause great financial loss, and even result in enormous human and property loss. Therefore, there is an urgent need to research fault control for electrical motor.

One of the potential failures in electrical motor is the stator current sensor fault. For electrical drive system, the measured stator currents are required for successful operation of the feedback control.

Generally, two current sensors are installed in conventional three-phase voltage-source inverters (VSI). Nevertheless, sudden severe failure of current sensors results in the over-current malfunction of the system, and if there is no protection scheme in the gate-drive circuit, it leads to irrecoverable faults of power semiconductors in the inverter, which causes degradation of motor drive performance. Moreover, the minor faults (such as gain drift and nonzero offset) of stator current sensor would result in torque pulsation synchronized with the inverter output frequency [1]. The larger offset and scaling error would bring about the worse performance of torque regulation. Ultimately, if the offset and gain drift are above a certain level, it would cause over-current trip at high speed and in heavy load

conditions [2]. So it is indispensable to solve the problem such that motor system is controlled to be disturbance-free under the faults of stator current sensor.

As for the aforementioned fault, there are two solution techniques, one being based-on hardware redundancy and the other based-on software—reconstructing stator currents (i.e., current sensorless method). Adding the redundant current sensor will increase higher cost and greater hardware complexity and bigger size drives. So the first solution is not cost effective and impracticable. Nowadays, digital signal processors have become more attractive as they have comparatively low-cost and can implement complex control strategies and therefore the second solution has been highly praising [3, 4, 5, 6, 7].

As for the current sensorless method, the most common technique first proposed by J.T.Boys [8] concentrates on adopting information from single current sensor in the DC-link of an inverter, which reconstructs stator currents according to the relationship between the DC-link current and stator currents. The drawback of the single current sensor technique is that on one hand, the duration of an active switching state may be so short that the DC-link current cannot be measured reliably. On the other hand, there are immeasurable regions in the output voltage hexagon where the current sampling and reconstruction is limited or impossible to do [9]. In addition, the technique may suffer from the very noisy of DC-link current feedback. In order to provide high-quality stator current reconstruction over a wide range of operating conditions with a low current waveform, Over the past years, many kinds of methods of improved PWM modulation strategy are proposed for the single current sensor technique [10-21]. Although many improvement methods show reasonable current reconstruction performance, these methods suffer from complicated algorithms to implement current estimation [22].

It is well-known that backstepping technique originated from Kanellakopoulos, Kokotovic and Morse [23] offers great flexibility in the synthesis of the control and the estimation of the variables for nonlinear system [24] and thus naturally lends itself to an adaptive extension to the case. It allows a good steady state and good dynamical behaviour in the presence of system parameters variation and disturbance. In order to avoid the disadvantage of abovementioned estimation method for stator current, in this paper, based on an adaptive backstepping, a novel observer used for reconstruction stator currents is proposed. Taking

stator resistance variation (due to heating during operating of the motor) into account, the designed observer is capable of concurrent estimation of stator current along dq-axis and stator resistance under the assumption that rotor speed and inverter output voltage as well as DC-link voltage are available. Compared to the previous technique, the proposed algorithm is less complicated and its implement is relatively easy.

Permanent magnet synchronous motor (PMSM) drives are nowadays widely used in the industry applications due to its capability of field-weakening control, its high efficiency and high power/torque density. For PMSM drives, the popular drive control strategies include two types: field oriented control strategy (FOC)[25] and direct torque control (DTC). Due to the inherent bandwidth of inner current loop, the dynamic response of FOC drive systems is limited. To improve the dynamic performance, DTC has recently begun to be applied. Compared to FOC, DTC directly manipulates the inverter's output voltage vector, hence eliminates the inherent delay caused by current loops and features comparatively good dynamic response. Even so, switching-table-based DTC presents some unavoidable drawbacks, such as high torque and flux ripples, variable switching frequency along with acoustic noise.

Apart from FOC and DTC, model predictive torque control (MPTC) is an emerging control concept and is received significant attention from electrical drives community [26-36] which adopts the principles of model predictive control (MPC) [37]. MPC has several merits such as easy inclusion of nonlinearities and constraints. Besides, its algorithm is simple and then its implementation is easy. Compared with previous two state-of-the art schemes, MPTC achieves more obvious reduction of the torque and flux ripples [38]. Furthermore, switching losses can be reduced [39]. Even so, MPTC has not yet been applied to current sensorless PMSM drive system. It is the abovementioned advantages of MPTC that motivates this paper.

For PMSM drives with the fault of stator current sensor, a novel current sensorless MPTC based on adaptive backstepping observer (ABO) is proposed. The proposed system can improve system performance and robustness.

The structure of the paper is as follows: modeling of PMSM is given in section two. In section three, the current sensorless MPTC system with ABO is established, and the ABO and MPTC are designed, respectively. The numerical simulation results & analysis and conclusion are reported in section four and five, respectively.

## 2 Dynamic Model of PMSM

As for three-phase PMSM, the model in rotor synchronous coordinate is expressed as follows,

$$\begin{cases} \frac{di_d}{dt} = \frac{1}{L_d}(u_d - R_s i_d + p\omega_r L_q i_q) \\ \frac{di_q}{dt} = \frac{1}{L_q}(u_q - R_s i_q - p\omega_r(L_d i_d + \Psi_m)) \end{cases} \quad (1)$$

Where

- $R_s$  resistance of the stator windings
- $L_d, L_q$  d-axis and q-axis stator inductance
- $\Psi_m$  permanent magnet flux
- $u_d, u_q$  d-axis and q-axis stator voltage
- $i_d, i_q$  d-axis and q-axis stator current
- $\omega_r$  mechanical rotor speed
- $p$  number of pole pairs

And mechanical equation is expressed as

$$\frac{d\omega_r}{dt} = \frac{1}{J}(T_e - T_l - B_m \omega_r - T_f) \quad (2)$$

Where

- $J$  inertia of moment
- $T_l$  load torque
- $B_m$  viscous friction coefficient
- $T_f$  coulomb friction torque
- $T_e$  electromagnetic torque, it can be expressed as

$$T_e = \frac{3p}{2} [\Psi_m i_q + (L_d - L_q) i_d i_q] \quad (3)$$

## 3 Design of Current Sensorless Model Predictive Torque Control Using Adaption Backstepping Observer

The objective of current sensorless MPTC based on ABO for PMSM drive system is that the drive control system not only can work reliably and its speed & torque can be controlled to not only have satisfactory performance but also be strong robust to stator resistance variation and external disturbance. The block diagram of current sensorless MPTC system based on ABO is designed as shown in Fig.1.

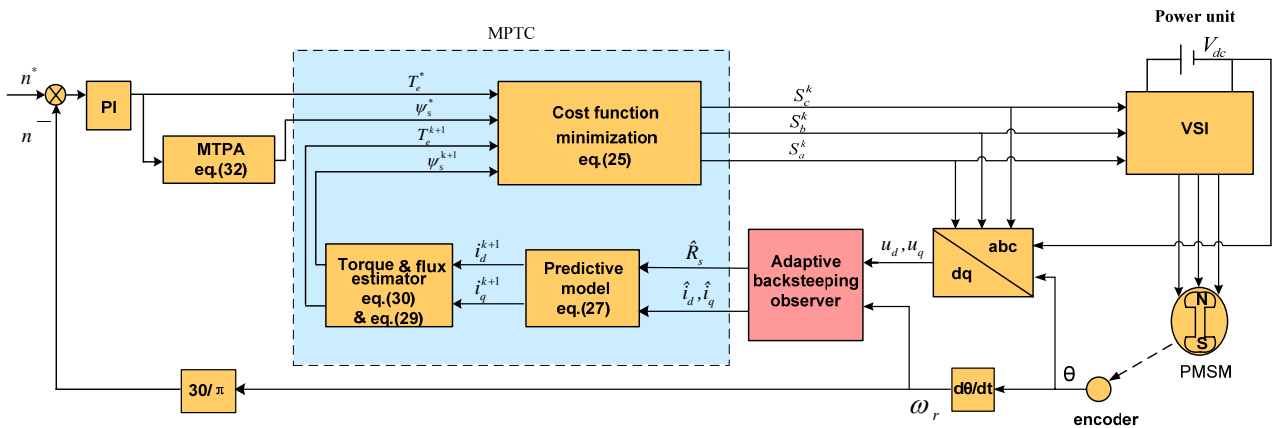


Fig. 1 Block diagram of current sensorless MPTC system based on ABO

It mainly comprises of five components: ABO, MPTC, Maximum Torque per Ampere (MTPA) (used for calculating reference stator flux linkage), Power unit and PI controller, respectively.

### 3.1 Adaptive backstepping observer

In this section, a novel observer based on nonlinear adaptive backstepping is proposed in case that neither of stator currents is available due to failure of stator current sensor under the assumption that rotor speed and inverter output voltage as well as DC-link voltage are available for measurement. All parameters of PMSM are considered as constant except stator resistance. The adaptive backstepping

observer can be used to estimate not only stator resistance but also stator currents.

For surface-mounted PMSM,  $L_d = L_q = L$ ,  $R_d = R_q = R_s$ . The observer is constructed as follows, which will be used to estimate stator currents and rotor speed.

$$\begin{cases} \frac{d\hat{i}_d}{dt} = \frac{1}{L}(u_d - \hat{R}_s \hat{i}_d + p\hat{\omega}_r \hat{L}_q) \\ \frac{d\hat{i}_q}{dt} = \frac{1}{L}(u_q - \hat{R}_s \hat{i}_q - p\hat{\omega}_r(\hat{L}_d + \Psi_m)) \end{cases} \quad (4)$$

$$\frac{d\hat{\omega}_r}{dt} = \frac{3p\Psi_m}{2J} \hat{i}_q - \frac{B_m}{J} \hat{\omega}_r - \frac{T_l}{J} \quad (5)$$

Where  $\hat{i}_d$ ,  $\hat{i}_q$  and  $\hat{\omega}_r$  are the estimation for dq-axis stator currents and speed, respectively. The stator resistance  $\hat{R}_s$  is considered as uncertain parameter with  $R_s$  as its nominal value.

From (4), it can be seen that the stator resistance to be estimated appears in the estimation of stator currents. In order to solve the stator currents and resistance tracking problem and overcome the difficulty that arises due to their coupling, the backstepping technique is adopted as following two steps:

**Step 1**

In the first step, we want to obtain the sufficient condition which can ensure that the system can track actual rotor speed trajectory.

Definite the stator currents tracking errors as following,

$$\begin{cases} e_d = \hat{i}_d - i_d \\ e_q = \hat{i}_q - i_q \end{cases} \quad (6)$$

And also definite the rotor speed tracking error as following,

$$e_\omega = \hat{\omega}_r - \omega_r \quad (7)$$

The dynamical equation of the speed estimation error, obtained by subtracting (2) from (5), is given by

$$\frac{de_\omega}{dt} = \frac{3p\Psi_m}{2J} e_q - \frac{B_m}{J} e_\omega \quad (8)$$

Let us check the stability of speed tracking error. By choosing candidate Lyapunov function below

$$V_1 = \frac{1}{2} e_\omega^2 \quad (9)$$

The time derivative of (9) is determined to be

$$\dot{V}_1 = e_\omega \left( \frac{3p\Psi_m}{2J} e_q - \frac{B_m}{J} e_\omega \right) \quad (10)$$

To render  $\dot{V}_1$  negative, we postulate the existence of following equality,

$$\frac{3p\Psi_m}{2J} e_q - \frac{B_m}{J} e_\omega = -k_\omega e_\omega \quad (11)$$

Where  $k_\omega$  is constant positive scalar.

It follows that

$$\dot{V}_1 = -k_\omega e_\omega^2 \quad (12)$$

Then we have  $\dot{V}_1 < 0$ , which guarantees that speed estimation error converges to zero. Moreover, from (11), we have q-axis stator current error as following

$$e_q = \frac{2J}{3p\Psi_m} (-k_\omega + \frac{B_m}{J}) e_\omega \quad (13)$$

Equation (13) is the sufficient condition that the estimation of speed can track actual one.

**Step 2**

In the second step, we try to obtain the sufficient condition which can ensure that the estimated stator currents could track the actual one. Meanwhile, stator resistance adaptive mechanism could be obtained.

Subtracting (1) from (4), the derivative of dq-axis current estimation errors take the following form

$$\begin{cases} \frac{de_d}{dt} = \frac{1}{L} (-\hat{R}_s e_d - \tilde{R}_s i_d + pL\hat{\omega}_r e_q + pLe_\omega i_q) \\ \frac{de_q}{dt} = \frac{1}{L} (-\hat{R}_s e_q - \tilde{R}_s i_q - pL\hat{\omega}_r e_d - pLe_\omega i_d - p\Psi_m e_\omega) \end{cases} \quad (14)$$

Where the resistance estimation error  $\tilde{R}_s = \hat{R}_s - R_s$ .

Choice candidate Lyapunov function below

$$V_2 = \frac{1}{2} (e_\omega^2 + e_q^2 + e_d^2 + \tilde{R}_s^2 / r) \quad (15)$$

Where r is constant positive scalar.

The candidate Lyapunov function derivative is as below

$$\begin{aligned} \dot{V}_2 = & -k_\omega e_\omega^2 - \frac{\hat{R}_s}{L} e_d^2 - \frac{\hat{R}_s}{L} e_q^2 + \tilde{R}_s \left( \frac{1}{r} \cdot \frac{d\tilde{R}_s}{dt} - \frac{1}{L} i_d e_d \right. \\ & \left. - \frac{1}{L} i_q e_q \right) + e_\omega (p i_q e_d - p i_d e_q - \frac{p\Psi_m}{L} e_q) \end{aligned} \quad (16)$$

To render  $\dot{V}_2$  negative, we postulate the existence of following two equalities,

$$\frac{1}{r} \cdot \frac{d\tilde{R}_s}{dt} - \frac{1}{L} i_d e_d - \frac{1}{L} i_q e_q = 0 \quad (17)$$

$$p i_q e_d - p i_d e_q - \frac{p\Psi_m}{L} e_q = -k'_\omega e_\omega \quad (18)$$

Where  $k'_\omega$  is constant positive scalar.

It follows that

$$\dot{V}_2 = -(k_\omega + k'_\omega) e_\omega^2 - \frac{\hat{R}_s}{L} e_d^2 - \frac{\hat{R}_s}{L} e_q^2 < 0 \quad (19)$$

Equation (19) guarantees that both (8) and (14) are stable. And (17) and (18) are the sufficient condition that the estimation error of stator currents converges to zero and does the estimation error of speed.

Furthermore, the variation of the stator resistance in the observer time scale is negligible, i.e.,

$$\frac{d\tilde{R}_s}{dt} = \frac{d\hat{R}_s}{dt} - \frac{dR_s}{dt} \approx \frac{d\hat{R}_s}{dt} \quad (20)$$

Thus from (17), the adaptive mechanism of stator resistance is derived as follows:

$$\hat{R}_s = \frac{r}{L} \int (i_d e_d + i_q e_q) dt \quad (21)$$

Taking (6) into account, (21) can be rewritten as following expression based on PI algorithm

$$\begin{aligned} \hat{R}_s = & \frac{r}{L} \left[ K_p \left( (i_d - e_d) e_d + (i_q - e_q) e_q \right) + \right. \\ & \left. K_I \int \left( (i_d - e_d) e_d + (i_q - e_q) e_q \right) dt \right] \end{aligned} \quad (22)$$

Where  $e_q$  can be obtained from (13), and  $e_d$  derived from (18) as follows

By combining (4), (5), (13), (22) and (23), the block diagram of the designed adaptive backstepping observer is constructed as shown in fig. 2, which

$$e_d = \frac{1}{p\hat{i}_q} (p\hat{i}_d e_q + \frac{p\Psi_m}{L} e_q - k'_\omega e_\omega) \quad (23)$$

treats the stator voltage vector and rotor speed as the inputs, the stator current vector and stator resistance as output.

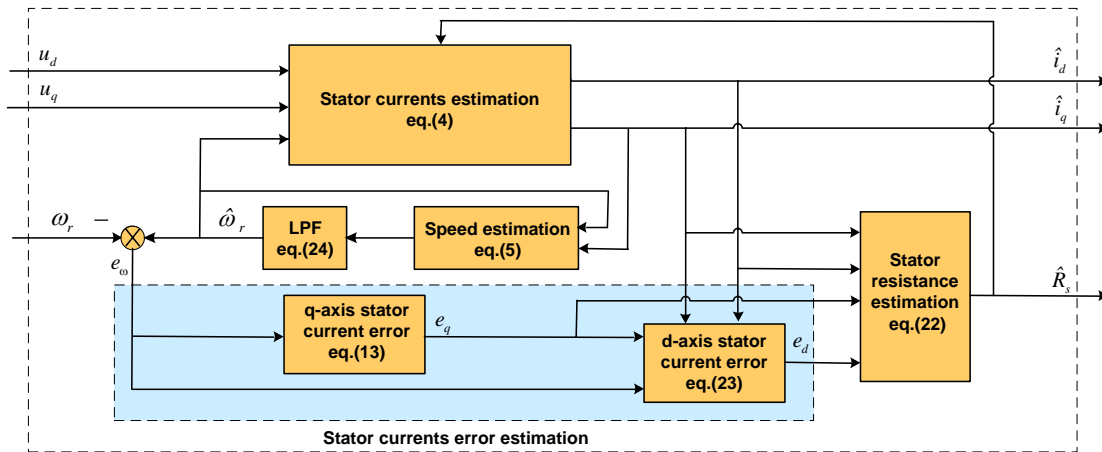


Fig. 2 Block diagram of the designed adaptive backstepping observer

**Remark 1.** The proposed ABO essentially is nonlinear and can be ensured to be asymptotically stable because its overall design process is based on Lyapunov stability theorem.

**Remark 2.** The estimation procedure needs to be based on the error of the speed generated from its measured and estimated value, which must be converged towards zero.

**Remark 3.** From fig.2, it can be seen that although the coupling relationship exists between  $\hat{i}_d$  and  $\hat{i}_q$  as well as between  $e_d$  and  $e_q$ , the design process saves the troubles of calculating decoupling of these variables involved. Without calculating decoupling, the estimation of stator resistance and stator currents ultimately can be obtained by backstepping technique. In fact, the current observer equations and the resistance adaptive law are implemented and solved all together.

**Remark 4.** Equation (23) presents singularity when  $\hat{i}_q$  approaches zero-crossing. The singularity elimination is managed by replacing  $\hat{i}_q = 0$  with a very small positive constant.

**Remark 5.** For more attenuation of noise, a low-pass filter (LPF) is used in speed estimation as shown in fig.2. The LPF adopts a first-order component as following

$$G(s) = \frac{1}{Ts + 1} \quad (24)$$

Where T is positive constant.

### 3.2 Model predictive torque control

The basic idea of MPTC is to predict the future behavior of the variables over a time frame based on the model of the system. In fact, MPTC is an extension of DTC, as it replaces the look-up table of DTC with an online optimization process in the control of machine torque and flux. Different from the employments of hysteresis comparators and switching table in conventional DTC, the principle of vector selection in MPTC is based on evaluating a defined cost function. The selected voltage vector from conventional switching table in DTC is not necessarily the best one in terms of reducing torque and flux ripples. There are limited discrete voltage vectors in the two-level inverter-fed PMSM drives, as a result, it is possible to evaluate the effects of each voltage vector and select the one minimizing the cost function.

As shown in fig.1, MPTC includes three parts: cost function minimization, predictive model and flux & torque estimators.

#### 3.2.1 Cost function minimization

For MPTC, the cost function is such chosen that both torque and flux at the end of the cycle is as close as possible to the reference value. Generally, the minimum value of cost function is defined as

$$\min .g = |T_e^* - T_e^{k+1}| + k_1 \left| |\Psi_s^*| - |\Psi_s^{k+1}| \right| \quad (25)$$

$$s.t. \quad u_s^k \in \{V_{1,2}, V_{2,2}, \dots, V_{5,2}, V_{6,2}\}$$

Where  $T_e^*$  and  $\Psi_s^*$  are reference values for torque and stator flux, respectively.  $T_e^{k+1}$  and  $\Psi_s^{k+1}$  predictions for torque and stator flux at  $k$ th instant, respectively.  $V_1, V_2, V_3, V_4, V_5,$  and  $V_6$  are six nonzero voltage space vectors and can be generated by healthy three phase inverter with respect to the different switches states. A set of voltage space vectors  $u_s^k$  at  $k$ th instant is defined as

$$u_s^k = 2V_{dc} \left[ S_a^k + e^{i2\pi/3} S_b^k + \left( e^{i2\pi/3} \right)^2 S_c^k \right] / 3 \quad (26)$$

Where  $S_x^k$  ( $x=a,b,c$ ) at  $k$ th instant is upper power switch state of one of three legs.  $S_x^k=1$  or  $S_x^k=0$  when upper power switch of one leg is on or off.  $k_l$  is the weighting factor. The selection of  $k_l$  is still an open problem for answer [19].

### 3.2.2 Predictive model for stator currents

According to (1), the prediction of the stator current at the next sampling instant is expressed as

$$\begin{cases} i_d^{k+1} = i_d^k + \frac{1}{L} (-R_s i_d^k + p\omega_r^k L i_q^k + u_d^k) T_s \\ i_q^{k+1} = i_q^k + \frac{1}{L} (-R_s i_q^k - p\omega_r^k L i_d^k - p\omega_r^k \Psi_m + u_q^k) T_s \end{cases} \quad (27)$$

Where  $T_s$  is the sampling period and  $\omega_r^k$  can be replaced by estimation speed  $\hat{\omega}_r^k$ .

### 3.2.3 Torque & flux estimators

In dq-system, the current-based flux-linkage  $\Psi_d$  and  $\Psi_q$  can be expressed as following vector [29]

$$\begin{bmatrix} \Psi_d^{k+1} \\ \Psi_q^{k+1} \end{bmatrix} = \begin{bmatrix} L & 0 \\ 0 & L \end{bmatrix} \begin{bmatrix} i_d^{k+1} \\ i_q^{k+1} \end{bmatrix} + \begin{bmatrix} \Psi_m \\ 0 \end{bmatrix} \quad (28)$$

The magnitude of stator flux linkage  $\Psi_s$  is

$$\Psi_s^{k+1} = \sqrt{\left( \Psi_d^{k+1} \right)^2 + \left( \Psi_q^{k+1} \right)^2} \quad (29)$$

Electromagnetic torque developed in dq-system can be estimated as following

$$T_e^{k+1} = \frac{3}{2} p \Psi_m i_q^{k+1} \quad (30)$$

Substituting (27) into (30), the torque can be estimated.

### 3.3 Maximum Torque per Ampere

According to the principle of maximum torque per Ampere, the reference stator flux linkage  $\Psi_s^*$  can be calculated as follows

$$\Psi_s^* = \sqrt{\left( T_e^* L / \frac{3}{2} p \Psi_m \right)^2 + \left( i_d^* L + \Psi_m \right)^2} \quad (31)$$

Where  $i_d^*$  is reference value of d-axis current and assumed to be zero, i.e.,

$$i_d^* = 0$$

As a result, the corresponding reference stator flux linkage  $\Psi_s^*$  is rewritten as

$$\Psi_s^* = \sqrt{\left( T_e^* L / \frac{3}{2} p \Psi_m \right)^2 + \Psi_m^2} \quad (32)$$

### 3.4 Power unit and PI controller

The power unit adopts 2-level 3-phase voltage source inverter. And PI controller is used to regulate the rotor speed [36].

## 4 Simulation Result and Analysis

In order to validate the effective of proposed control scheme, the designed control system from fig.1 has been implemented in Matlab/Simulink/Simscape platform. The parameters of PMSM are given in Table 1. In order to verify the good tracking effect of the estimated values and the satisfactory control performance of the current sensorless MPTC scheme, two scenarios of numerical simulation are given and compared, which correspond to MPTC with current sensor and based-observer MPTC without current sensor, respectively.

Table1 Parameters of PMSM

Symbol	Quantity	Value
$R_a, R_b, R_c$	Nominal phase resistance	2.875Ω
$L_d, L_q$	dq-coordinate inductance	0.0085H
$\Psi_m$	Rotor magnetic flux	0.175Wb
$p$	Number of pole pairs	4
$V_{dc}$	DC bus voltage	300V
$n_N$	Rated speed	2000rpm
$T_n$	Rated torque	4Nm
$J$	Moment of inertia	0.0008Kg.m <sup>2</sup>
$B_m$	Viscous friction coefficient	0.001Nms
$T_f$	Coulomb friction torque	0

The sampling period is 10 μ s; the value  $k_l$  is selected to be 200. The parameters of PI in MPTC for two scenarios are selected as follows,

$$K_p = 0.6, K_i = 0.2$$

As for the observer, the parameters of PI in stator resistance estimation (22) are

$$K_p = 0.02, K_i = 8.8$$

And other parameters of the observer are respectively selected as

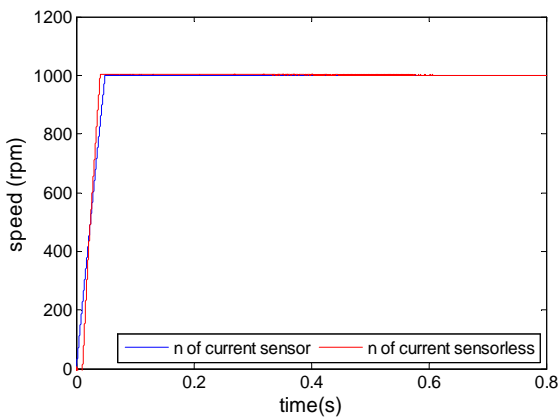
$$k_{\omega} = k'_{\omega} = 0.01, r = 1, T = 1/80$$

For above-mentioned two scenarios, figs. 3(a)-3(m) show their comparison results in terms of rotor speed, torque, stator currents in abc-system & dq-system, estimated stator resistance and trajectory of stator flux linkage when the reference speed  $n^*$  is set to 1000 rpm, the load torque of 4Nm.

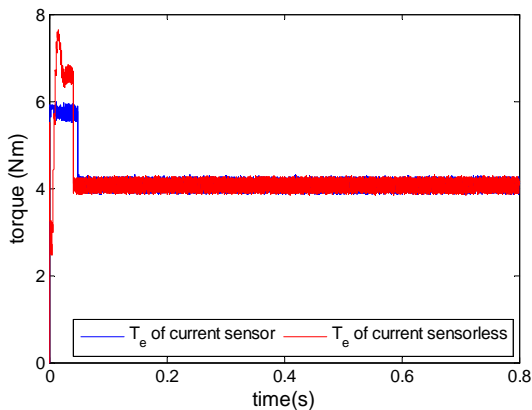
In the case of the variation of stator resistance, figs. 4(a)-4(m) display the comparison of two scenarios. In the simulation, the stator resistance of nominal value  $2.875 \Omega$  is changed to  $3.5 \Omega$  at 0.5 seconds.

In the case of the load variation, figs. 5(a)-5(m) show the comparison of two scenarios. In the simulation, the load torque of 4Nm is changed to 2 Nm at 0.3seconds and late restored to 4Nm at 0.5 seconds.

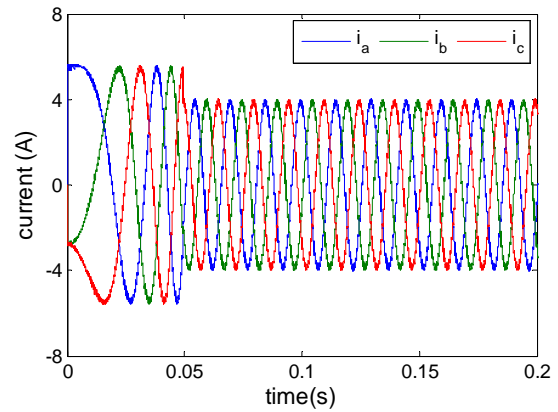
In the case of the variation of speed change, figs. 6 (a)-6 (m) show the comparison of two scenarios. In the simulation, reference speed  $n^*$  of 1000 rpm is changed to 600 rpm at 0.5 seconds.



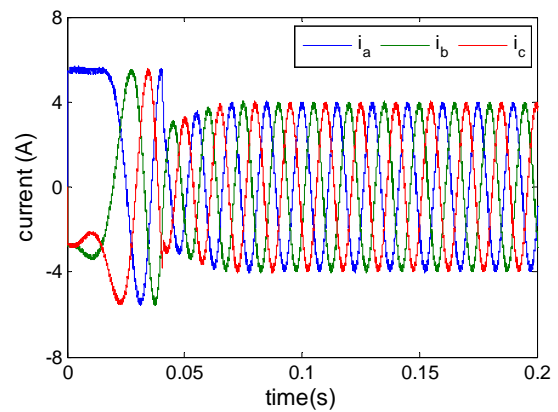
(a) Rotor speed response



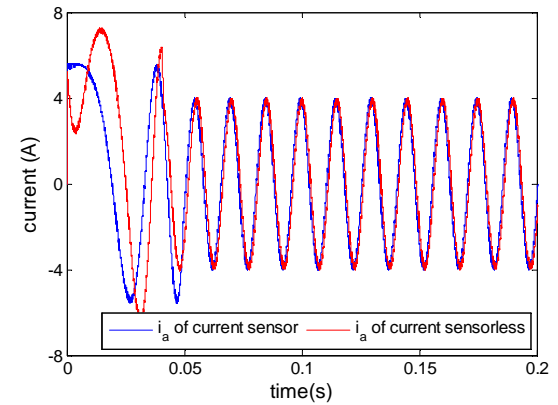
(b) Torque response



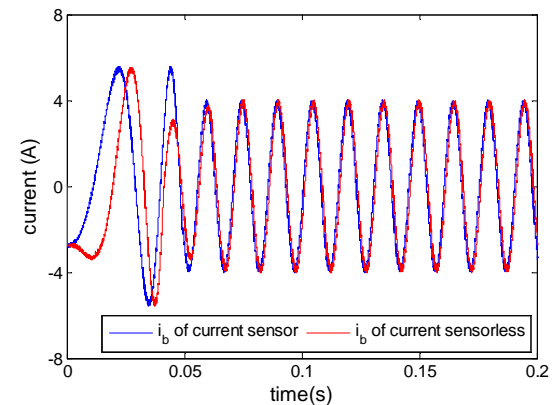
(c) Stator currents in abc-system with current sensor



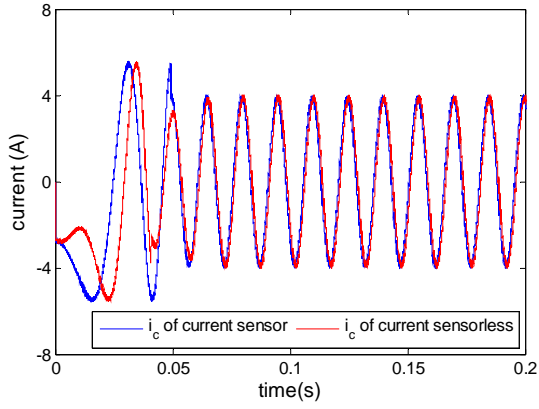
(d) Stator currents in abc-system with current sensorless



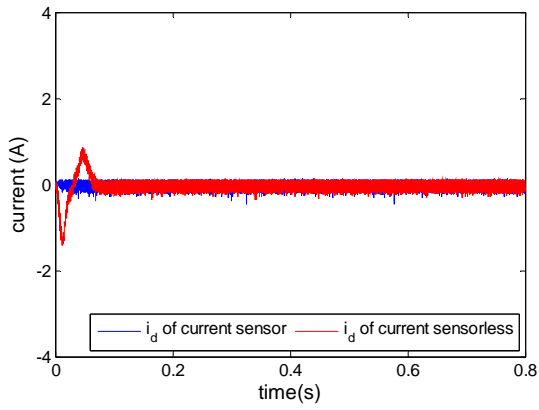
(e) Stator currents  $i_a$



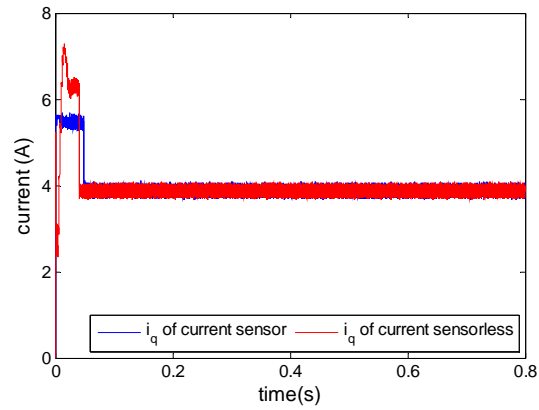
(f) Stator currents  $i_b$



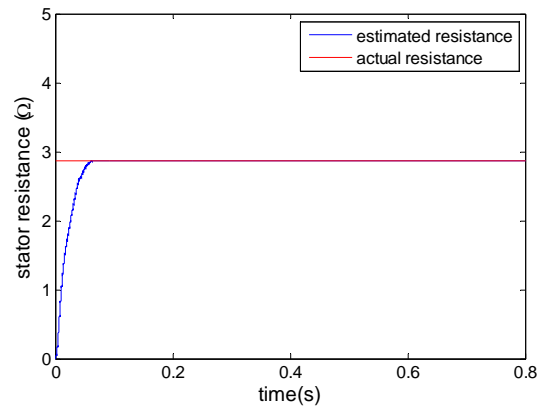
(g) Stator currents  $i_c$



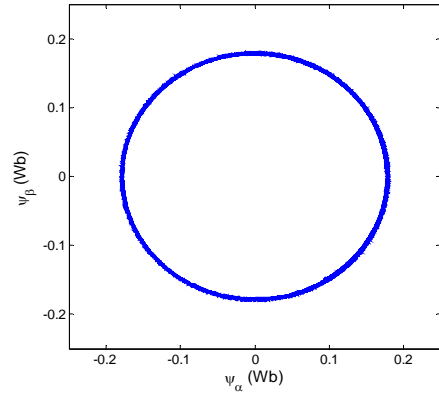
(h) d-axis stator currents  $i_d$



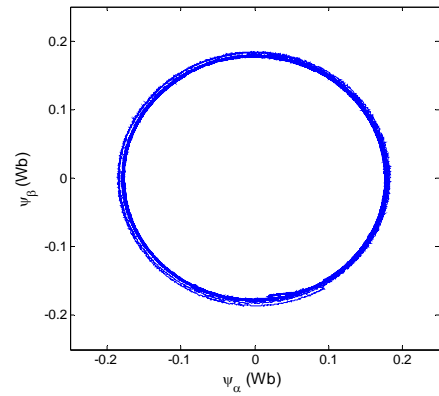
(i) q-axis stator currents  $i_q$



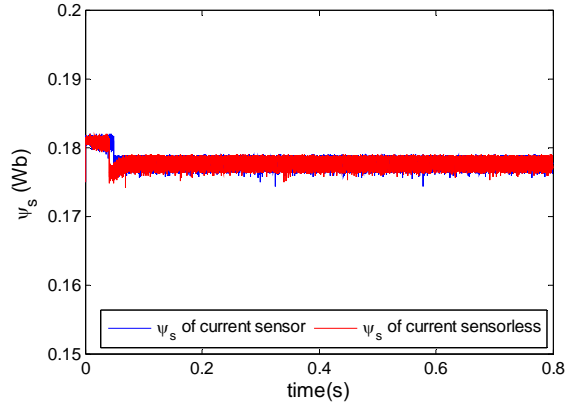
(j) Estimated and actual stator resistance



(k) Trajectory of stator flux linkage for MPTC with current sensor



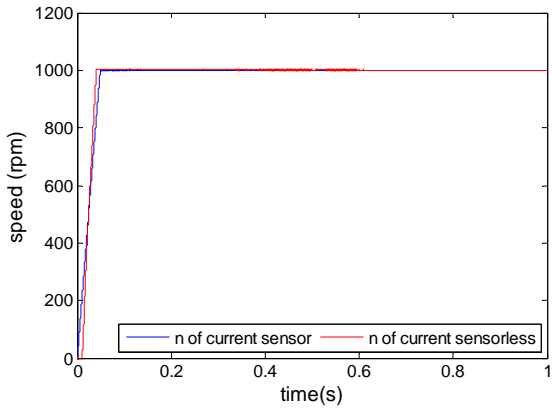
(l) Trajectory of stator flux linkage for MPTC with current sensorless



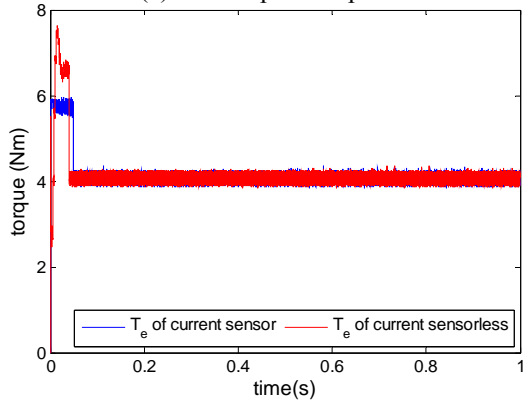
(m) Stator flux linkage  $\psi_s$

Fig.3 Dynamic response comparison between MPTC with current sensor and MPTC with current sensorless

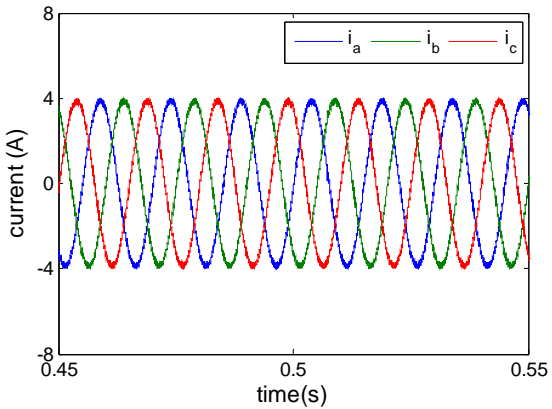




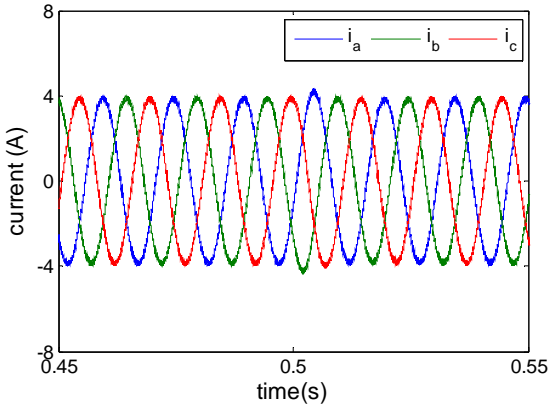
(a) Rotor speed response



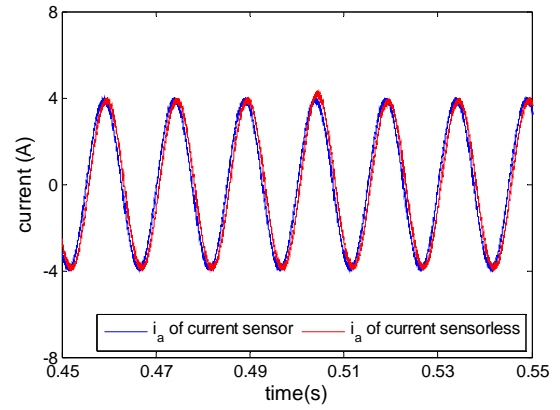
(b) Torque response



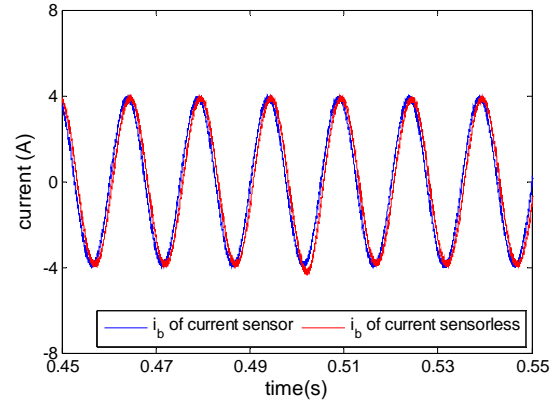
(c) Stator currents in abc-system with current sensor



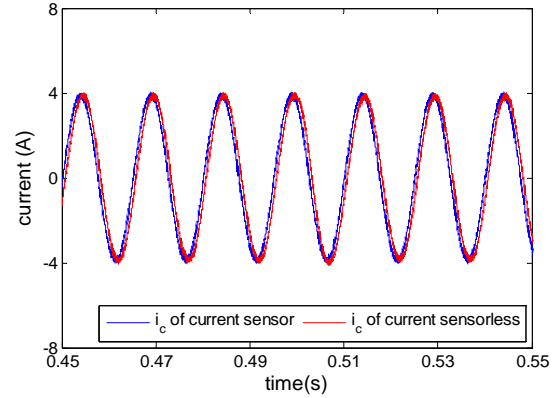
(d) Stator currents in abc-system with current sensorless



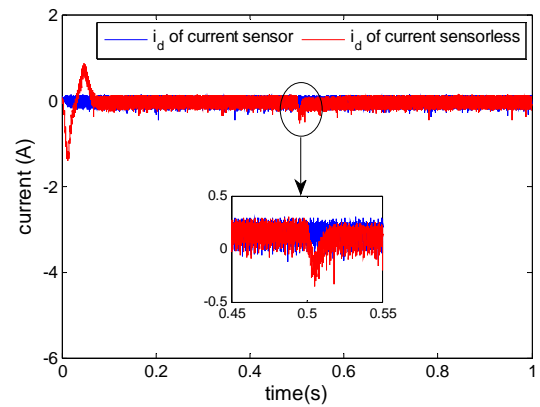
(e) Stator currents  $i_a$



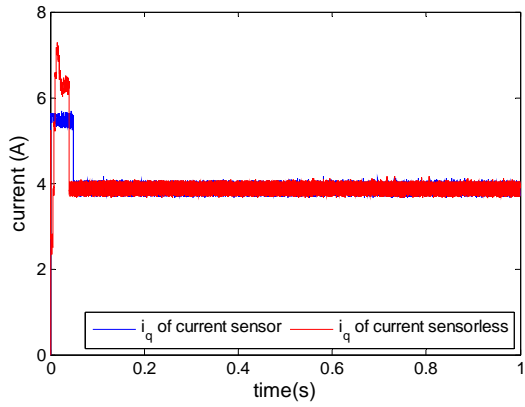
(f) Stator currents  $i_b$



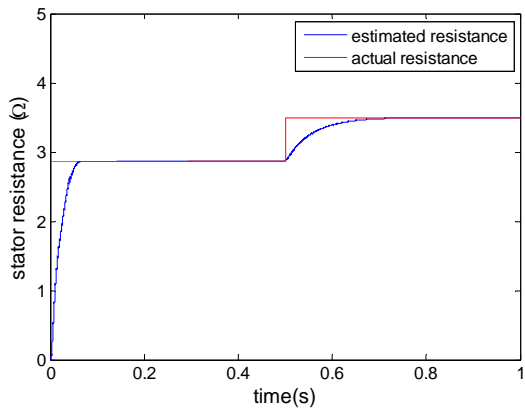
(g) Stator currents  $i_c$



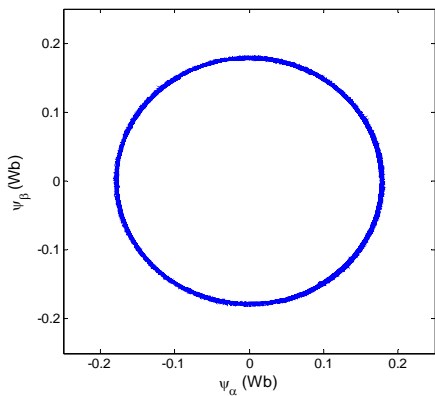
(h) d-axis stator currents  $i_d$



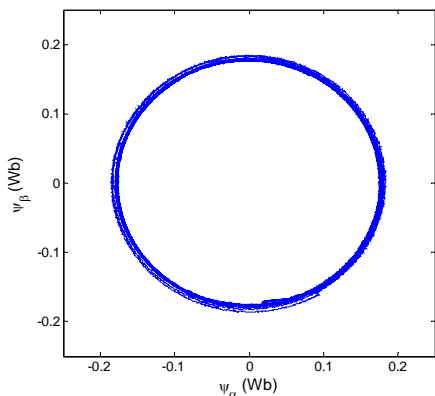
(i) q-axis stator currents  $i_q$



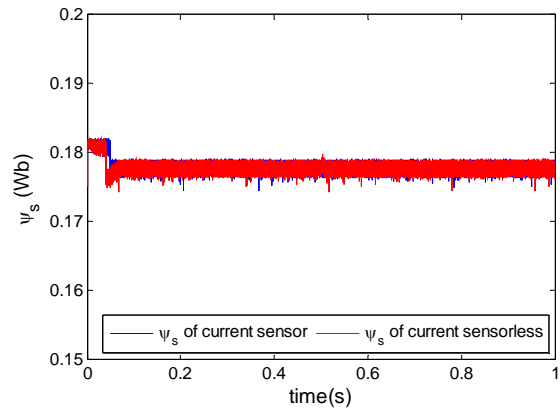
(j) Estimated and actual stator resistance



(k) Trajectory of stator flux linkage for MPTC with current sensor

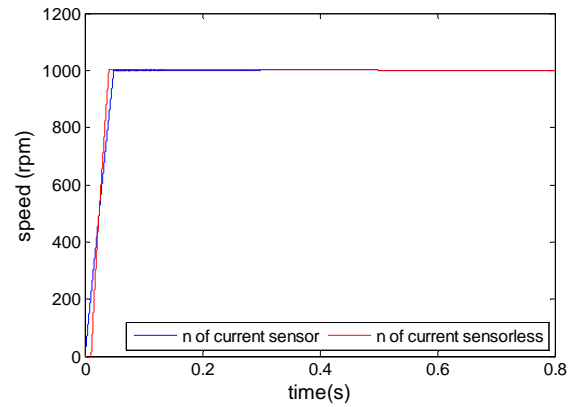


(l) Trajectory of stator flux linkage for MPTC with current sensorless

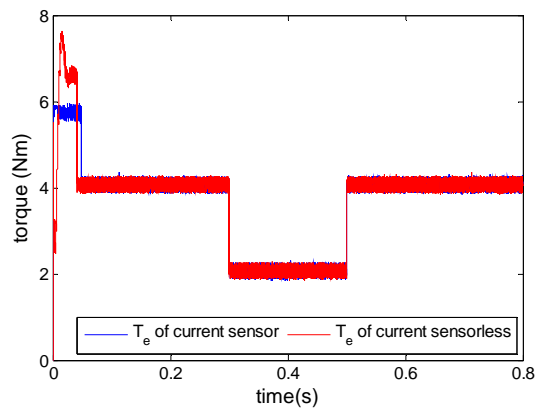


(m) Stator flux linkage  $\psi_s$

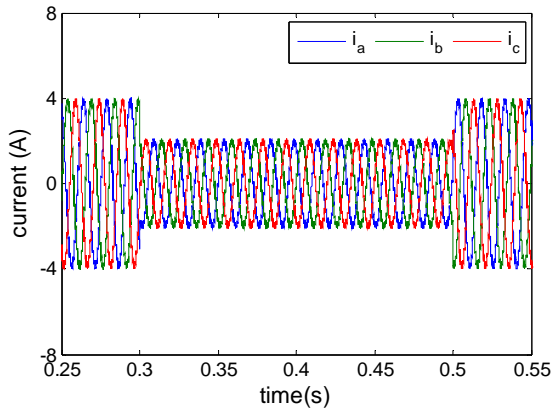
Fig.4 Dynamic response comparison between MPTC with current sensor and MPTC with current sensorless in the case of stator resistance variation



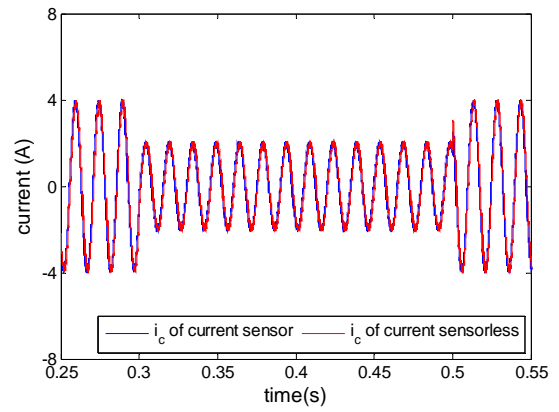
(a) Rotor speed response



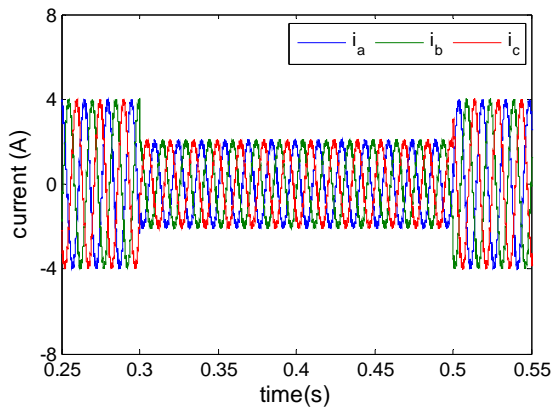
(b) Torque response



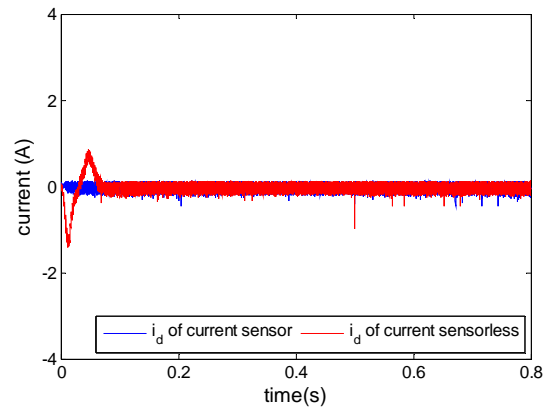
(c) Stator currents in abc-system with current sensor



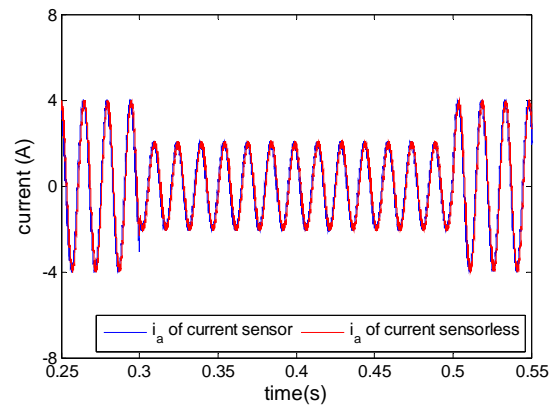
(g) Stator currents  $i_c$



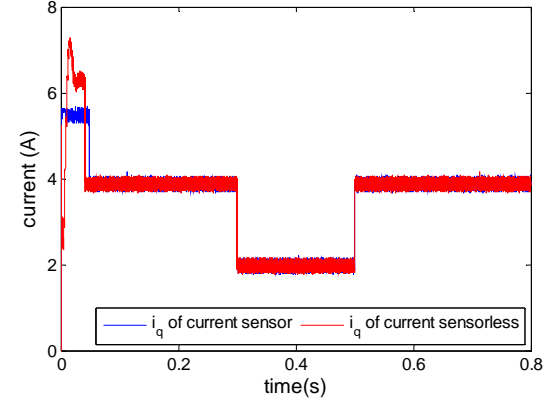
(d) Stator currents in abc-system with current sensorless



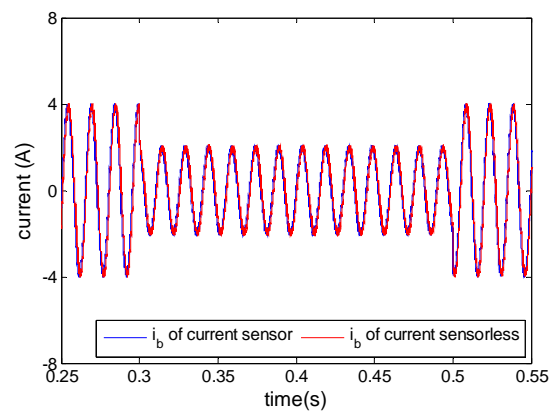
(h) d-axis stator currents  $i_d$



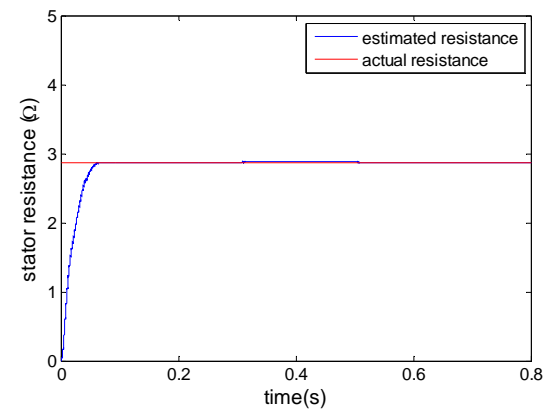
(e) Stator currents  $i_a$



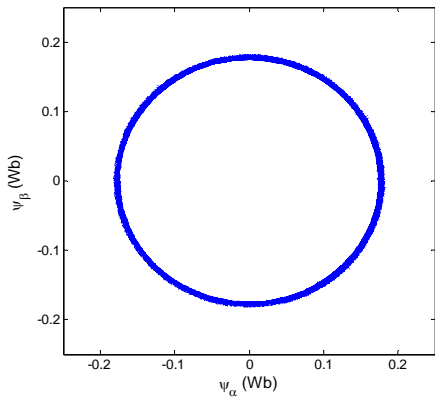
(i) q-axis stator currents  $i_q$



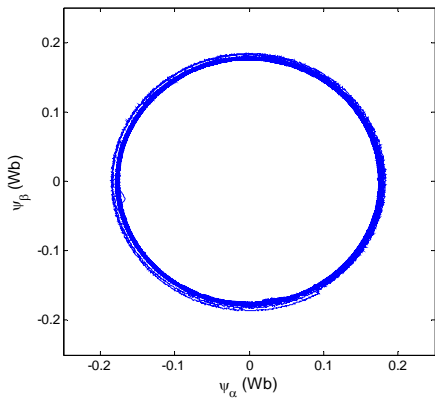
(f) Stator currents  $i_b$



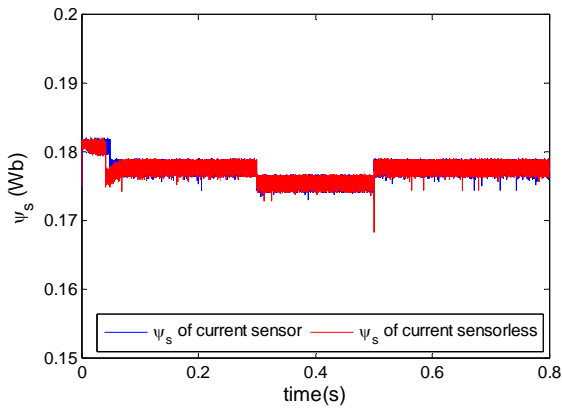
(j) Estimated and actual stator resistance



(k) Trajectory of stator flux linkage for MPTC with current sensor

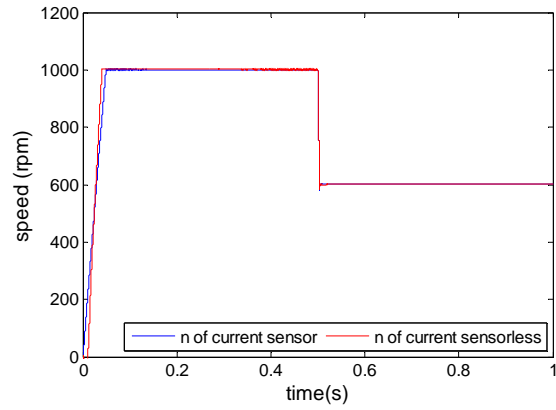


(l) Trajectory of stator flux linkage for MPTC with current sensorless

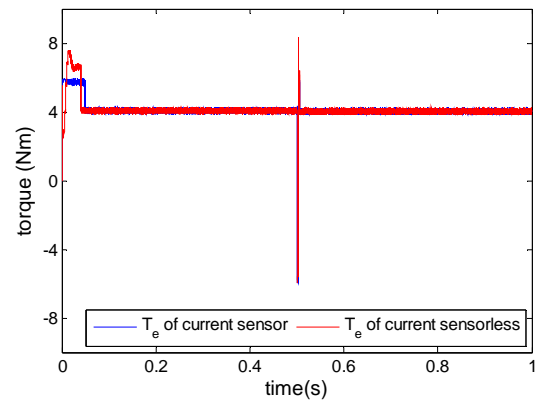


(m) Stator flux linkage  $\psi_s$

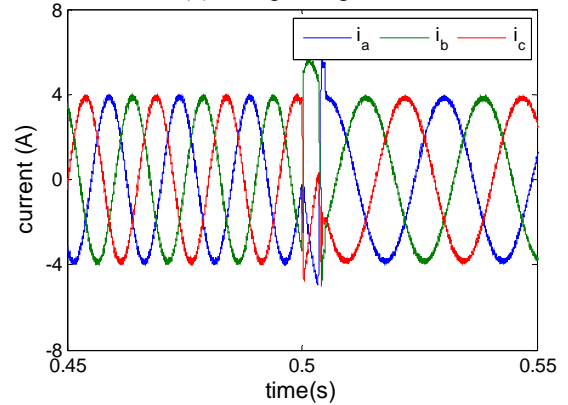
Fig.5 Dynamic response comparison between MPTC with current sensor and MPTC with current sensorless in the case of load torque change



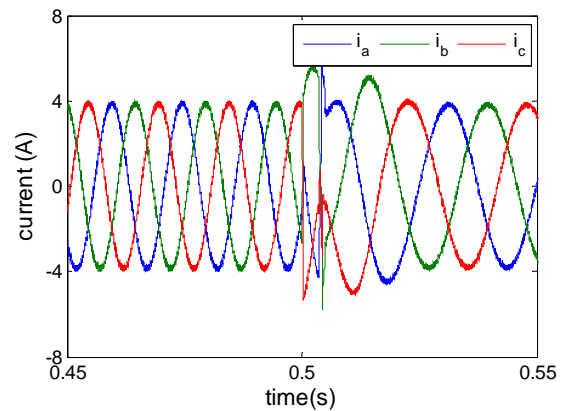
(a) Rotor speed response



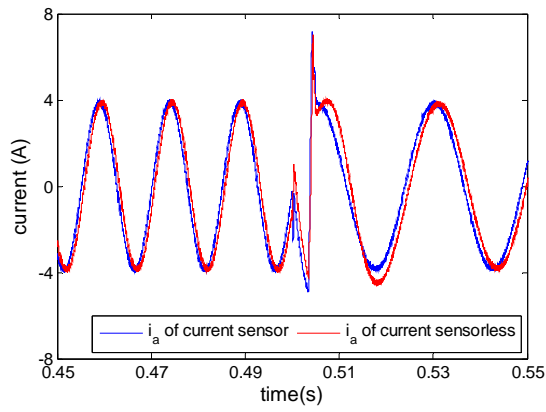
(b) Torque response



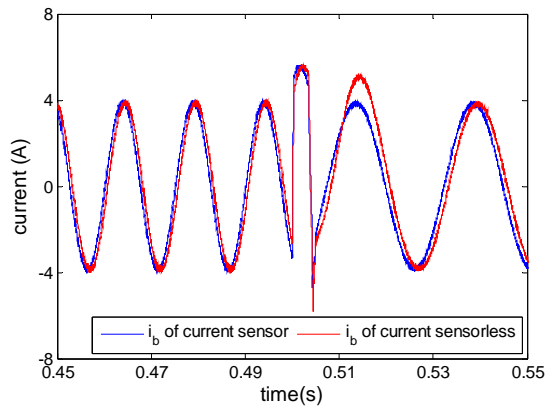
(c) Stator currents in abc-system with current sensor



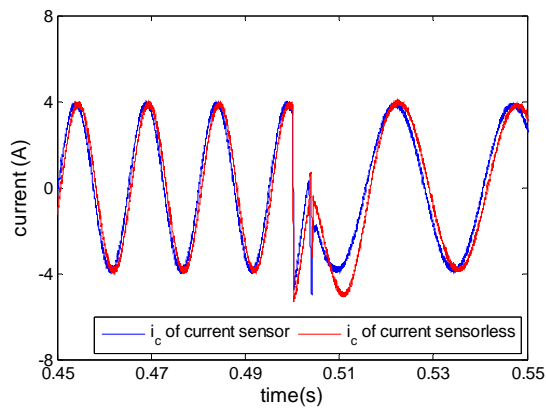
(d) Stator currents in abc-system with current sensorless



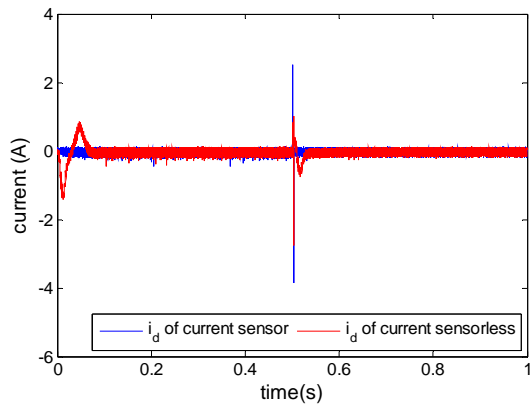
(e) Stator currents  $i_a$



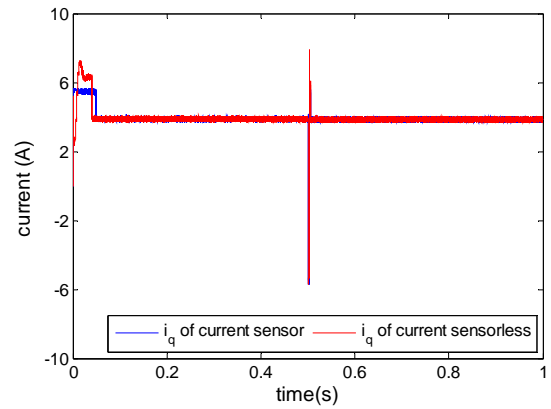
(f) Stator currents  $i_b$



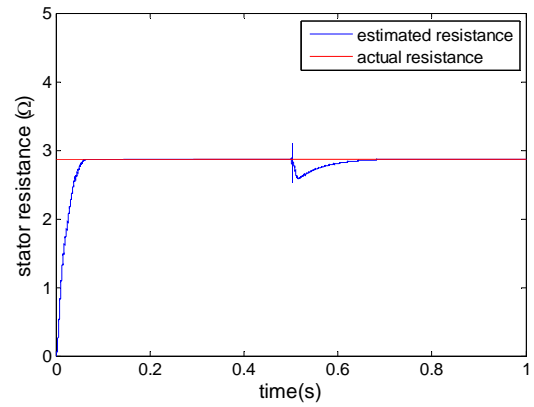
(g) Stator currents  $i_c$



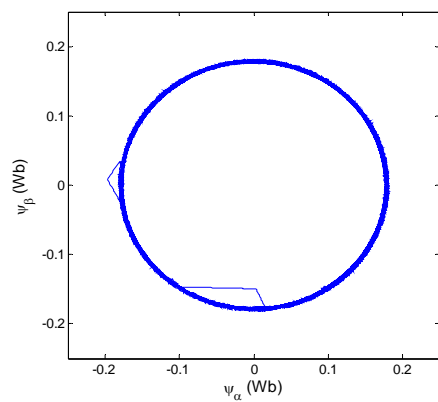
(h) d-axis stator currents  $i_d$



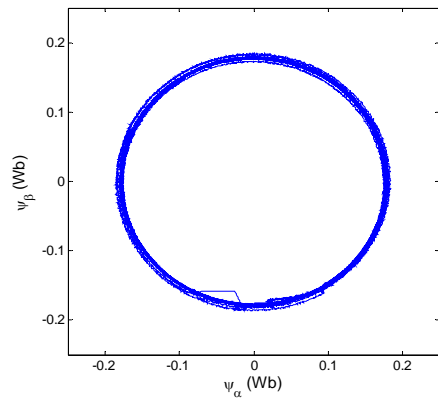
(i) q-axis stator currents  $i_q$



(j) Estimated and actual stator resistance



(k) Trajectory of stator flux linkage for MPTC with current sensor



(l) Trajectory of stator flux linkage for MPTC with current sensorless

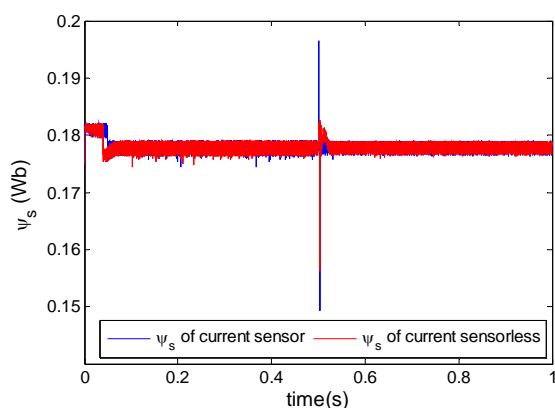
(m) Stator flux linkage  $\Psi_s$ 

Fig.6 Dynamic response comparison between MPTC with current sensor and MPTC with current sensorless in the case of speed change

Analyzing these simulations, the following consequence could be obtained:

- It can be seen from figs. 3 (a) -3 (m) that current sensorless MPTC system based on ABO is stable and have almost as good performance as MPTC system with current sensor. And the estimated stator currents can track actual ones of MPTC with current sensor and the estimated stator resistance can converge to the given nominal value accurately.
- As far as the resistance variation of PMSM is concerned, it can be seen from figs. 4 (a) -4 (m) that its estimated value can rapidly track actual change of PMSM and thus the ability against resistance variation of the proposed MPTC strategy without any current sensor is strong.
- As for external load variation, it can be seen from figs. 5 (a) -5 (m) that the generated electromagnetic torque can adapt to the change of external load and the capable of accommodating the challenge of load disturbance of the proposed MPTC strategy without any current sensor is strong.
- As far as the speed variation of PMSM is concerned, it can be seen from figs. 6 (a) -6 (m) that the accuracy of speed tracking is high and the ability to deal with reference speed change is strong.

To sum up, the proposed current sensorless MPTC based on ABO can make PMSM drive

system to have not only satisfactory control performance but also strong robustness.

## 5 Conclusion

This paper has puts forward a novel current sensorless MPTC scheme based on ABO for three-phase PMSM drive system without any current sensor. Making use of the technique of adaptive backstepping, the observer is designed which is capable of concurrent online estimation of stator current and stator resistance under the assumption that rotor speed and inverter output voltage as well as DC-link voltage are available for measurement. Stability and convergence of the observer are analytically verified based on Lyapunov stability theory. In order to reduce the torque & flux ripples and improve drives control performance, MPTC strategy is employed. The proposed algorithm is less complicated and its implement is relatively easy. It can ensure that the drives system achieves satisfactory torque & speed control and strong robustness. Extensive simulation validates the feasibility and effectiveness of the proposed scheme.

## References:

- [1] D. Chung and S. Sul, "Analysis and compensation of current measurement error in vector-controlled AC motor drives," *IEEE Trans. Ind. Appl.*, vol. 34, no. 2, pp. 340-345, Mar./Apr. 1998.
- [2] Y.S. Jeong, S.K. Sul, E. Schulz, and N.R. Patel, "Fault Detection and Fault-Tolerant Control of Interior Permanent-Magnet Motor Drive System for Electric Vehicle," *IEEE Trans. Ind. Appl.*, vol. 41, no. 1, pp. 46-51. Jan./Feb. 2005.
- [3] Q.F.Teng and D. W. Fan, "Robust Hinf Reliable Control with Exponential Stabilization for Uncertain Delay Systems against Sensor Failure," *Electric Machines and Control*, vol. 12, no.2, pp.195-201, 2008.
- [4] Q.F.Teng and D. W. Fan, "Robust Fault-tolerant Control via State Observer for Uncertain Systems with Delay," *Dynamics of Continuous Discrete and Impulsive Systems--series B--Applications and Algorithms*, pp.382-386, 2006.
- [5] Q.F.Teng and D. W. Fan, "Guaranteed Cost Reliable Control with Exponential Stabilization for Uncertain Time-varying Delayed Systems," *Systems Engineering and Electronics*, vol.30,no. 3, pp.530-534,2008.
- [6] C. Axenie, "A New Approach in Mobile Robot Fault Tolerant Control," *WSEAS Transactions*

- on Systems and Control*, vol. 5, no. 4, pp. 205-216, 2010.
- [7] Q.F.Teng, J.G. Zhu, T. S. Wang, G. Lei, "Fault Tolerant Direct Torque Control of Three-Phase Permanent Magnet Synchronous Motors," *WSEAS Transactions on systems*, vol.11,no.11,pp.465-476, 2012.
- [8] J. T. Boys, "Novel current sensor for PWM ac drives," in *IEE Proceedings: Electric Power Applications*, vol. 135, pp. 27-32,1988.
- [9] H.Y. Ma, K. Sun, Q. Wei, and L. P. Huang, "Phase current reconstruction for AC motor adjustable speed drives in the over modulation method," *Journal of Tsinghua University*, vol.50, no.11, pp. 1757-1761, 2010.
- [10] T.C. Green, B.W. Williams, "Derivation of motor line-current waveforms from the DC-link current of an inverter," in *IEE Proceedings, Part B: Electric Power Applications*, vol.136, no.4, pp. 196-204,1989.
- [11] H. Kim, and T. M. Jahns, "Phase Current Reconstruction for AC Motor Drives Using a DC Link Single Current Sensor and Measurement Voltage Vectors," *IEEE Trans. on Power Electronics*, vol.21,no.5, pp.1413-1419, 2006.
- [12] J. Ha, "Voltage Injection Method for Three Phase Current Reconstruction in PWM Inverters Using a Single Sensor," *IEEE Trans. on Power Electronics*, vol.24, no.3, pp. 767-775, 2009.
- [13] J. Ha, "Current Prediction in Vector Controlled PWM Inverters Using Single DC-Link Current Sensor," *IEEE Trans. on Industrial Electronics*, vol.57, no.2, pp.716-726, 2010.
- [14] K. Sun, Q. Wei, L. P. Huang, and K. Matsuse, "An Over modulation Method for PWM Inverter Fed IPMSM Drive With Single Current Sensor," *IEEE Trans. on Industrial Electronics*, vol.57, no.10, pp.3395-3404, 2010.
- [15] Y.K. Gu, F. L. Ni, D. P Yang, and H. Liu, "Switching State Phase Shift Method for Three Phase Current Reconstruction with a Single DC-Link Current Sensor," *IEEE Trans. Ind. Electr.*, vol.58, no.11, pp. 5186-5194, 2011.
- [16] B. Metidji, N. Taib, L. Baghli, T. Rekioua, and S. Bacha. "Low Cost Direct Torque Control Algorithm for Induction Motor Without AC Phase Current Sensors," *IEEE Trans. on Power Electronics*, vol.27, no.9, pp. 4132-4139, 2012.
- [17] Y.S. Lai, Y.K. Lin, and C.W. Chen. "New Hybrid Pulse width Modulation Technique to Reduce Current Distortion and Extend Current Reconstruction Range for a Three-Phase Inverter Using Only DC-link Sensor," *IEEE Transactions on Power Electronics*, vol.28, no.3, pp.1331-1337,2013.
- [18] H.F. Lu, X. M. Cheng, W.L. Qu, S. Sheng, Y. T. Li, and Z.Y. Wang. "A Three-Phase Current Reconstruction Technique Using Single DC Current Sensor Based on TSPWM," *IEEE Trans. on Power Electronics*, vol.29,no.3, pp.1542-1550, 2014.
- [19] Y. Gu, F. Ni, D. Yang, J. Dang, and H. Liu, "Novel method for phase current reconstruction using a single dc-link current sensor," *Electric machine and control*, vol.13,no.6, pp. 811-816, 2009.
- [20] W. Wang, M. Cheng, B.F.Zhang, Y. Zhu, and S.C. Ding, "Fault-tolerant Control Focusing on Phase Current Sensors of Permanent Magnet Synchronous Machine Drive Systems Based on Hysteresis Current Control," in *Proceedings of the CSEE*, vol.32, no.33, Nov.25, 2012
- [21] H. F. Lu, X. M. Cheng, W.L. Qu, S. Sheng, Y.T. Li, and Z.Y. Wang, "A Three-Phase Current Reconstruction Technique Using Single DC Current Sensor Based on TSPWM," *IEEE Trans. on Power Electronics*, vol.29, no.3, pp.1542-1550, 2014.
- [22] Y.H. Cho, T. LaBella, and J. Lai, "A Three-Phase Current Reconstruction Strategy With Online Current Offset Compensation Using a Single Current Sensor," *IEEE Trans. on Industrial Electronics*, vol.59, no.7, pp. 2924-2933, 2012
- [23] I.Kanellakopoulos, P.V.Kokotovic and A.S.Morse, "Systematic Design of Adaptive Controllers for Feedback Linearizable Systems," *IEEE Trans. Automat. Contr.*, vol.36, pp.1241-1253, 1991.
- [24] F. Neri, "Quantitative Estimation of Market Sentiment: a discussion of two alternatives," *WSEAS Transactions on Systems*, vol. 11, no. 12, pp.691-702, 2012.
- [25] A.M.Yang, J.P.Wu, W.X.Zhang, and X.H. Kan, "Research on Asynchronous Motor Vector Control System Based on Rotor Parameters Time-varying," *WSEAS Transactions on Systems*, vol. 7, no. 4, pp.384-393, 2008.
- [26] S. Kouro, P. Cortes, R. Vargas, U. Ammann, and J. Roriguez, "Model Predictive Control—A Simple and Powerful Method to Control Power Converters," *IEEE Trans. on Industrial Electronics*, vol.56, no.6, pp. 1826-1838, 2009.
- [27] H. Miranda, P. Cortes, J.I. Yuz, and J. Rodriguez, "Predictive torque control of induction machines based on state-space

- models,” *IEEE Trans. Industry Electronics*, vol.56, no.6, pp.1916-1924, 2009.
- [28] M.Preindl, and S. Bolognani, “Model Predictive Direct Torque Control with Finite Control Set for PMSM Drive Systems, Part 2: Field Weakening Operation,” *IEEE Trans. on Industrial Informatics*, vol.9, no.2, pp.648-657, 2013.
- [29] R. P.Aguilera, P. Lezana, and D. E. Quevedo, “Finite- Control-Set Model Predictive Control With Improved Steady-State Performance,” *IEEE Trans. on Industrial Informatics*, vol.9, no.2, pp. 658-667, 2013.
- [30] T. Geyer, “Model Predictive Direct Current Control: Formulation of the Stator Current Bounds and the Concept of the Switching Horizon,” *IEEE Trans. Ind. Appl.*, vol.18, no. 2, pp.47-59, 2012.
- [31] T. Geyer, “A Comparison of Control and Modulation Schemes for Medium-Voltage Drives: Emerging Predictive Control Concepts Versus PWM-Based Schemes,” *IEEE Trans. Ind. Appl.*, vol.47, no.3, pp.1380-1389, 2011.
- [32] T.Geyer, “Model Predictive Direct Torque Control—Part I : Concept, Algorithm, and Analysis,” *IEEE Trans. Ind. Electr.*, vol.56, no.6, pp.1894-1905, 2009.
- [33] Y. Zhang, W. Xie, Z. Li, and Y. Zhang, “Model Predictive Direct Power Control of a PWM Rectifier With Duty Cycle Optimization,” *IEEE Trans. on Power Electronics*, vol.28, no.11, pp.1007-1015, 2013.
- [34] M. Preindl , and S. Bolognani, “Model Predictive Direct Speed Control with Finite Control Set of PMSM Drive Systems,” *IEEE Trans. on Power Electronics*, vol.28, no.2, pp.1007-1015, 2013.
- [35] S. Chai, L. Wang, and E. Rogers, “A Cascade MPC Control Structure for a PMSM With Speed Ripple Minimization,” *IEEE Trans. Ind. Electr.*, vol.60, no.8, pp.2978-2987, 2013.
- [36] Q.F. Teng, J.Y.Bai, J.G.Zhu, Y.X. Sun, “Fault Tolerant Model Predictive Control of Three-Phase Permanent Magnet Synchronous Motors,” *WSEAS Transactions on systems*, vol.8, no.12, pp.385-397, 2013.
- [37] C.E.Garcia, D.M.Prett, and M. Morari, “Model predictive control: Theory and practice— A survey,” *Automatica*, vol.25, no.3, pp.335-348,1989.
- [38] Y.C.Zhang, J.G.Zhu, W.Xu, “Predictive torque control of permanent magnet synchronous motor drive with reduced switching frequency,” in *International Conference on Electrical Machines and Systems (ICEMS)*, pp.798-803, 2010.
- [39] T. Geyer, “Generalized model predictive direct torque control: Long prediction horizons and minimization of switching losses,” In *proc. IEEE Conf. Decis. Control*, Shanghai, China, pp.6799-6804, Dec.2009.